Journal of Applied Polymer Science

Preparation and Properties of β-Phase Graphene Oxide/PVDF Composite Films

Ningli An, Shaolong Liu, Changqing Fang, Ruien Yu, Xing Zhou, Youliang Cheng
The Department of Packaging Engineering, Institute of Printing and Packaging Engineering, Xi'an University of Technology, Xi'an 710048, Shaanxi, China
Correspondence to: C. Fang (E-mail: fcqxaut@163.com)

ABSTRACT: We report preparation of graphene oxide (GO) from expanded graphite (EG) via a modified Hummers method. GO/PVDF composites films were obtained using solvent N, N-Dimethylformamide (DMF) and cosolvent comprising deionized water/DMF combination. X-ray diffraction (XRD) and Fourier transform infrared spectroscopy (FTIR) analyses revealed that the main crystal structure of the composite films is β-phase, and use cosolvent method tends to favor the formation of β-phase. Scanning electron microscopy (SEM) was used to investigate the microstructure of composite films. Storage modulus and loss modulus were measured by Dynamic mechanical analysis (DMA). Broadband dielectric spectrum tests showed an increase in the dielectric constant of the GO/PVDF composite films with the rising content of GO, and by cosolvent method could improve the dielectric constant while reducing the dielectric loss. Our method that uses GO as an additive and deionized water/DMF as the cosolvent provides a promising and low-cost pathway to obtain high dielectric materials. © 2014 Wiley Periodicals, Inc. J. Appl. Polym. Sci. **2015**, *132*, 41577.

KEYWORDS: composites; crystallization; dielectric properties; surfaces and interfaces; X-ray

Received 30 May 2014; accepted 1 October 2014
DOI: 10.1002/app.41577

INTRODUCTION

In recent years, with the development of microelectronics devices and nanoscale electronic devices, dielectric materials have come increasingly to the research community's attention. Based on materials properties, dielectric materials can be divided into two types, inorganic polymer composites and organic polymer composites.[1] The traditional high dielectric materials are ferroelectric ceramics materials, such as barium titanate ($BaTiO_3$) and lead titanate ($PbTiO_3$),[2] the high dielectric loss, low breakdown voltage and low resistance of these materials have limited their development in the field of energy storage. By comparison, the organic polymer materials have drawn increasing attention due to the good processability, high breakdown strength (100–900 KV/mm) and low dielectric loss (10^{-4}) of these materials.[3]

PVDF is a highly crystalline fluoropolymer that belongs to a class of tough thermoplastics, which exhibit good electrochemical activity and thermal stability.[4] Generally speaking, PVDF exists in four crystalline phases: α, β, γ, and ε phase[5] and the first three types are common. As shown in Figure 1(a), the α-phase is the most common crystal structure that forms during solution processing of PVDF. Figure 1(b) shows the β-phase which has a trans planar zigzag structure (TTTT), that leads to the largest spontaneous polarization per unit cell in comparison with other crystal phases, contributing to the material's high pryo- and piezo-electric properties.[6,7] In Figure 1(c), the γ-phase (TTGTTTGT) is shown that may be obtained from both solution and melt-crystallization at temperatures above 160°C.[8] Among these crystalline phases, the β-phase is the most attractive PVDF crystal type, which has the highest ferro- and piezoelectric properties with the largest spontaneous polarization and can be used for a variety of applications.[9–11] Therefore, much attention has been paid to the research and development of the β-phase PVDF.

Graphene oxide (GO) is currently of great interest due to its low cost, easy availability, and its widespread ability to be converted into graphene. The scalability of this material is also a very desirable feature.[12,13] The usual way for preparing GO is Hummers method that includes proportional amounts of oxidants, such as potassium permanganate, sodium nitrate, and concentrated sulfuric acid that are mixed in a specified order with the graphite.[14]

The addition of nanofillers to PVDF is often performed aiming at the nucleation of the electroactive β-phase.[15] Layek et al.[16] prepared poly (methyl methacrylate)-functionalized graphene/PVDF nanocomposites and found that graphene sheets enhanced β-polymorph PVDF formation, while increasing the thermal stability of the nanocomposites. To observe the influences of nanocarbon sheets on the electrical performance of PVDF, Song et al.[17] studied the dielectric properties of graphene/PVDF composites. They discovered that when the quality

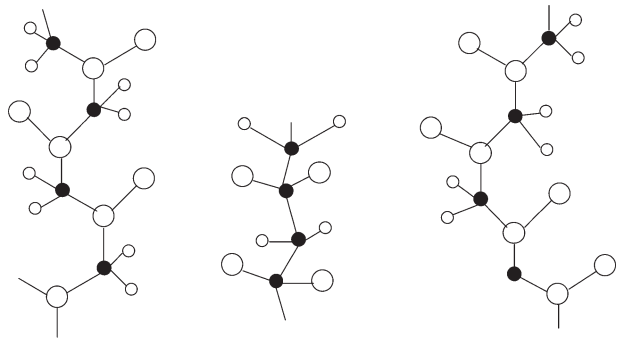

Figure 1. The crystal structure (a) the α- phase, (b) the *β*- phase, and (c) the *γ*- phase of PVDF(●: carbon atom; O: fluorine atom; ○: hydrogen atom).

ratio of graphene was 0.25%, the dielectric constant of the composite was 1.7 times greater than pure PVDF.

Subsequently, GO has been used to prepare PVDF membranes. Wang et al.[18] dissolved GO and PVDF in DMF to prepare organic-inorganic-blended ultrafiltration membranes. The GO-blended PVDF membranes appeared to be more hydrophilic, and the tensile strength was also significantly enhanced. Kuwahara et al.[19] demonstrate electro-luminescence enhancement by the addition of GO nanosheets as a comparatively high dielectric additive for PVDF, PVA, etc. Their study shows that the optimal volume of GO is 2.5 wt %, and the dielectric constant of the composites increased by more than 10-fold and enhanced the electroluminescence to more than three times that of the composite layer with 1.0 wt % of GO. Sigamani et al.[20] used a cosolvent approach involving water and DMF to dissolve GO and PVDF, to obtain the GO/PVDF composites. The cosolvent approach helped to disperse GO in a high aspect ratio in the PVDF matrix. Dielectric results showed that with the addition of GO remarkably increased the electrical conductivity of the composites.

Currently, use of GO as filler for modifying polymers has focused primarily on the mechanical properties and thermal performance.[21] Research on the microstructure and dielectric properties are relatively scarce. This article introduces the preparation for *β*-phase GO/PVDF composite films and the PVDF crystalline phase transition. Additionally, preliminary investigations were conducted on the dielectric properties and dielectric mechanism of GO/PVDF composite films. By controlling the content of GO and deliberating whether to add deionized water into the solvent, a series of GO/PVDF composite films were prepared. Herein we present and discuss our investigations of the crystalline phases, mechanical properties and the dielectric properties.

EXPERIMENTAL

Materials

N, N-Dimethylformamide (DMF) was purchased from the Tianjin FuYu Chemical PVDF, as the film material, was obtained from the Shanghai 3F NewMaterials (FR-904). Expanded graphite (EG, expansion rate = 200 mL/g) was obtained from Qingdao Haida Graphite (Qingdao, China). Deionized water.

Preparation of Graphene Oxide (GO)

GO was prepared by a modified Hummers method from EG (Expanded Graphite). 2 g of EG and H_2SO_4 (98%, 100 mL) were placed in a bottom-round flask. $KMnO_4$ (10 g) was added in an ice-water bath with continuously stirring. The mixture was stirred for 2.5 h at 10°C, and then stirred continuously for another 1.25 h in a thermostatic waterbath (35°C). Deionized water (400 mL) and H_2O_2 (30%, 5 mL) was then added with continuous stirring to prevent effervescing that resulted in a bright yellow suspension. The suspension was subsequently washed with diluted hydrochloric (1 : 10), and then dispersed the suspension in the deionized water (200 mL) by ultrasonic. Take dodecyl amine (3 g) dissolved in anhydrous ethanol (100 mL) and stir to make it fully dissolved. After which the dissolving liquid was added to the graphene oxide suspension, and stirred for 48 h at 50°C to obtain the amination of GO dispersion solution. Finally, the dispersion solution was washed with ethanol six times and then kept in a vacuum oven (60°C) for 24 h to obtain a dry GO.

Solution Preparation

GO/PVDF solutions were prepared by solution composite method.

1. GO (0.01 g) was suspended in DMF (100 mL), stirring and intermittent ultrasonic dispersion were continued throughout the process for 5 h at 60°C (made into the solution of the mass fraction of 0.01%) to ensure the suspension stable and uniform, with 0.0001 g of GO in per milliliter solution.
2. The samples were distributed as six groups according to the different ration of GO and different solvent, shown in Table I.

Preparation of the Nanocomposite Films

The specific process of composite films preparation is listed as follows (ultrasonic power is 100 W):

1. Dissolve quantitative PVDF in DMF solution, stirring and ultrasonic for 1 h, until the PVDF solution became transparent.
2. Measuring quantitative GO/DMF solution (Sample C need to add 2 mL deionized water into GO/DMF solution, then stirring and ultrasonic for 1 h at 40°C). Add PVDF/DMF solution to GO/DMF solution, stirring, and ultrasonic the mixed solution for 2 h at 45°C.
3. The well-dispersed GO/PVDF nanocomposites are placed on a glass substrate in the vacuum drying oven at 120°C for 3 h to evaporate solvent, well below the melting temperature of PVDF.
4. Decrease the temperature in the vacuum drying oven at the rate of 10°C/15 min, until the temperature is below 40°C.
5. Peeling off these composite films from the glass substrate, and then coating a circular conductive aluminum layer as electrode on these composite films for dielectric performance test.

Characterization

X-ray Diffraction (XRD). XRD was performed using a XRD-7000 diffractometer (SHIMADZU LIMITED, Japan) with two-

Table I. Samples and Formulations

Samples	Solution	GO
A	PVDF(1 g)/DMF	0
B1	PVDF(0.9996 g)/DMF/4 mLGO	0.04 wt %
B2	PVDF(0.9994 g)/DMF/6 mLGO	0.06 wt %
B3	PVDF(0.9992 g)/DMF/8 mLGO	0.08 wt %
B4	PVDF(0.9990 g)/DMF/10 mLGO	0.1 wt %
C[a]	PVDF(0.9990 g)/DMF/ 10 mLGO/2 mL deionized water	0.1 wt %

[a] GO/PVDF nanocomposite films are synthesized by cosolvent method involving deionized water and DMF.

dimensional (2D) area detector with Cu K*a* radiation. The diffraction patterns of GO/PVDF composite films in the 2θ range of 10–70° and the peaks corresponding to the α- and β-phase polymorphic modification were detected.

Fourier Transform Infrared Spectroscopy (FTIR). To identify the α- and β-phase polymorphic modification of PVDF, a Fourier Transform IR spectrophotometer [SHIMADZU FTIR-8400S (CE)] and recorded in the transmission mode at room temperature by averaging 20 scans was utilized to perform a FTIR analysis on the GO/PVDF composite film samples. The spectra were analyzed in the frequency range of 1000–400 cm^{-1}.

Dynamic Mechanical Analysis (DMA). The dynamic mechanical analysis was used in tensile mode at a frequency of 1 Hz, and the static force is 0.01*N*. The blended films were made in the form of rectangular strips having dimensions of 30 mm × 10 mm × 0.05 mm, approximately. After heating from −45 to 80°C at rate of 5°C/min, the storage modulus, loss factor and tanδ as a function of the temperature were recorded.

Scanning Electron Microscopy (SEM). Surface morphology of the impact fracture was analyzed by means of SEM. The fraction surfaces of sample were coated with a layer of gold by a JFC-1600 Sputter coater for 5 min. The SEM experiments were performed by a JSM-6390A scanning electron microscopy to observe the morphology of the dispersed phase.

Dielectric Properties. The dielectric properties of samples were measured with a frequency range between 10^{-2} and 10^{-7} Hz at room temperature using a Novocontrol Technologies Broadband dielectric spectrum test system (Concept 80, Novocontrol, Germany), used to analyze dielectric constant and dielectric loss.

RESULTS AND DISCUSSION

XRD Analysis

The crystalline phase analysis of the experimental samples was carried out using the X-ray diffraction (XRD). In general, PVDF powder was mainly composed of α-phase, Figure 2(a) shows the XRD of α-phase PVDF, the strong peaks appear at $2\theta = 18.5°$ and 27° indicating the α-phase.[22]

As shown in Figure 2(b), the XRD spectrum of PVDF was measured at a temperature of 120°C. It can be seen that at 120°C, $2\theta = 18.5°$ on behalf of the diffraction peak of α- and γ- phase is restrained, $2\theta = 27°$ diffraction peak decreased significantly corresponding to the α-phase. This illustrates that at 120°C, with the addition of GO, the α-phase in the crystal is restrained and large amounts of β-phase existed in the crystal structure.

Figure 3(a) shows XRD of pure PVDF film and GO/PVDF films with the GO content of 0.04%, 0.06%, 0.08%, and 0.1% sequentially. It shows that the α- and γ-phase of these crystalline structure of the composite films are suppressed, this implies that with the addition of GO at the crystallization temperature of 120°C, β-phase formation is favored.

Figure 3(b) shows the XRD of the GO/PVDF films with the GO content of 0.1%. It can be seen that in curve C, $2\theta = 18.5°$ corresponding to the diffraction peaks of α- and γ- phase is obviously weaker than curve B4, and in curve C exhibits less volatility than curve B4. This indicates that the cosolvent method for the synthesis of GO/PVDF nanocomposites, which involved addition of deionized water and DMF, can convert α-phase to β-phase, resulting in a further increase of β-phase in crystal. This may occur from addition of deionized water which disperses the GO more uniformly in the mixed solution, thus reducing the formation of a microporous structure during the preparation of the composite film. This improves the stability of the framework, thus affecting the physical properties of the material.

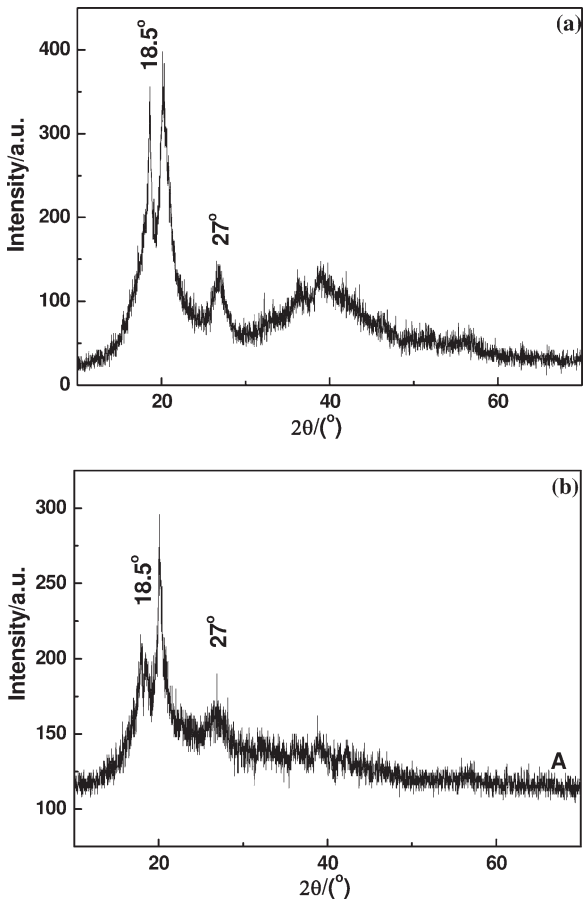

Figure 2. XRD spectrum of (a) α-phase and (b) β-phase of PVDF.

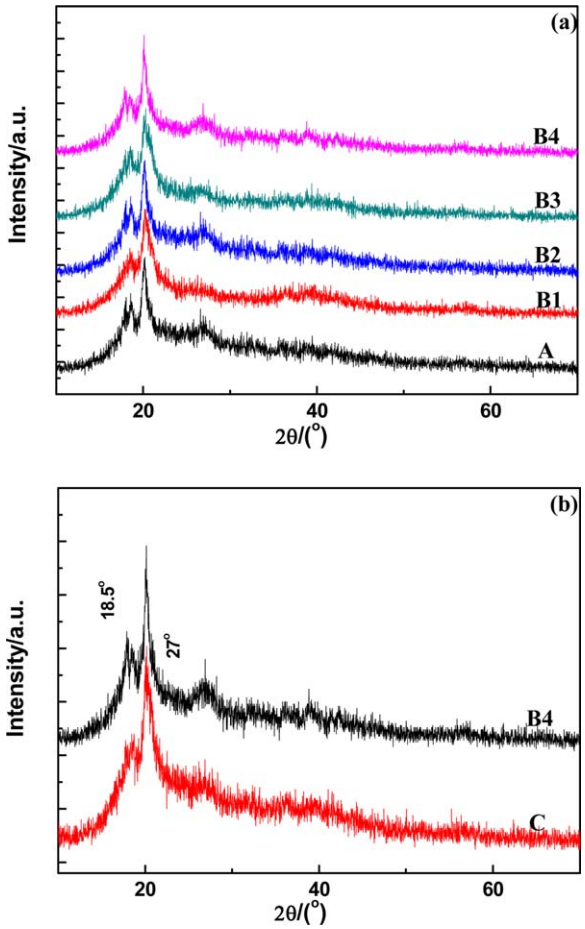

Figure 3. XRD spectrum of the GO/PVDF composite films with (a) (A) 0, (B1) 0.04, (B2) 0.06, (B3) 0.08, (B4) 0.10 and (b) (B4) 0.10, (C) 0.10 (cosolvent method DMF+ water) wt % GO. [Color figure can be viewed in the online issue, which is available at wileyonlinelibrary.com.]

FTIR Analysis

Figure 4(a) shows the FTIR spectra of GO/PVDF composite films. The peaks at 530 cm^{-1}, 610 cm^{-1}, 765 cm^{-1}, 975 cm^{-1} are related to the α-phase, and the peaks at 440 cm^{-1}, 840 cm^{-1}, 510 cm^{-1} can be assigned to the β-phase. The presence of the β-phase in PVDF films indicates strong dielectric properties and piezoelectric properties. The peaks at 430 cm^{-1} are related to the γ-phase.[23]

As we can see from Figure 4(a), the peak representing the β-phase of curve A (PVDF) and B4 (0.1% GO/PVDF) at 440 cm^{-1} is relatively weaker, peaks of α-phase at 610 cm^{-1}, 765 cm^{-1}, 975 cm^{-1} are slightly stronger than other curves. We observe in Figure 4(b), appearance of the peak at 440 cm^{-1} that was not discussed by previous investigators. This peak makes its appearance in the spectra of PVDF films comprising a substantial fraction of the β-phase, which demonstrates strong piezoelectric properties. The spectrum demonstrates a broad and peak located at 440 cm^{-1} and 840 cm^{-1} are related both to the β-phase of PVDF. Compared with B4, curve C the peaks at 840 cm^{-1} and 440 cm^{-1} corresponding to the β-phase peaks are enhanced and the peaks of α-phase at 610 cm^{-1} and 975 cm^{-1} are slightly reduced.

FTIR and XRD tests provided similar results. These results indicate that the transition from the metastable β-phase to the stable α-phase was prevented by the homogeneous dispersion of GO nanoparticles in the PVDF matrix owing to the match of crystal lattice of GO with the β-phase of PVDF, which is similar to the effect of adding clay to obtain the β-phase of PVDF.[24] Hydrogen bonds were formed between the hydroxyl group on the surface of the GO particles[25] and the polar C—F bonds of the PVDF.[26] The movement and arrangement of the polymer chains were restricted and oriented to the surface of GO to form an orderly arrangement. This mechanism induces formation of the β-phase of PVDF at 120°C. Using the cosolvent approach involving deionized water and DMF helps to disperse GO with high aspect ratio in the PVDF matrix and then affect the crystalline structure of PVDF, continuing to shift the α-phase towards to the β-phase.

Dynamic Mechanical Analysis

Dynamic Mechanical Analysis (DMA) is an effective and important technique for the analysis of polymer molecular chains, structure, and properties. Figure 5 shows the temperature

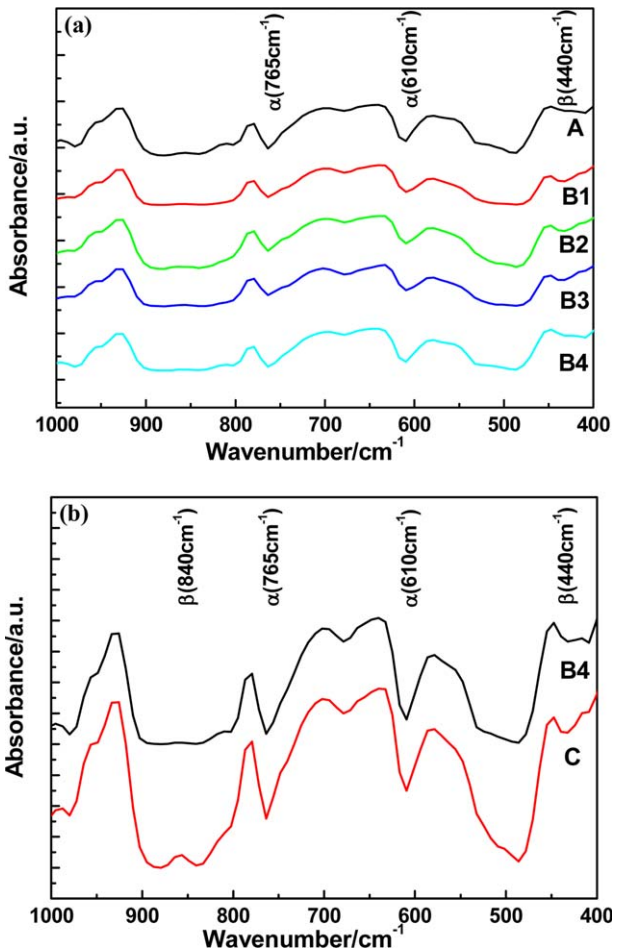

Figure 4. FTIR of the GO/PVDF composite films with (a) (A) 0, (B1) 0.04, (B2) 0.06, (B3) 0.08, (B4) 0.10 and (b) (B4) 0.10, (C) 0.10 (cosolvent method DMF+ water) wt % GO. [Color figure can be viewed in the online issue, which is available at wileyonlinelibrary.com.]

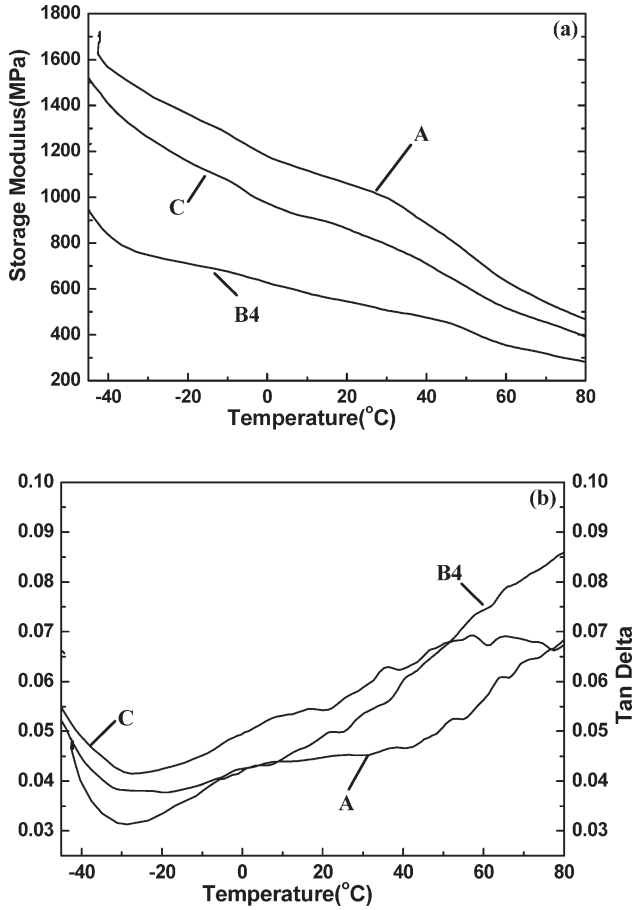

Figure 5. DMA spectrum (a) storage modulus and (b) loss factor of (A) 0, (B4) 0.10, (C) 0.10 (cosolvent method DMF+ water) wt % GO.

dependence of the storage modulus and the loss factor of the GO/PVDF composite films, at 1 Hz.

In Figure 5(a), compared with pure PVDF films, the storage modulus (E') of composite films decreased with the addition content of GO. This is due to the facts that GO did not combine well with the PVDF in composite structure and the addition of GO destroyed the PVDF crystal structure, leading to a drop in storage modulus. It is can be inferred that the rigidity of composite films is lower than the pure PVDF films. For curve C, the energy storage modulus of GO/PVDF composite films which was prepared by the cosolvent deionized water/DMF method is improved in comparison with curve B4, this reveals that in the composite interface the combination between GO and PVDF has improved, and in macro presentation exhibit the increase of storage modulus.

Figure 5(b) shows the loss factor ($\text{Tan}\delta = E''/E'$) of the composite films. Since the glass transition temperature (T_g) of PVDF is between -42°C and -5°C, we can infer that the Tanδ peak between -20°C and -5°C is the glass transition peak of PVDF. With the addition of GO, the glass transition peak shifts to a higher temperature. This is due to the fact that PVDF is a semi-crystalline polymer, where GO changes the movement of PVDF molecular chains, and thus the glass transition temperature changes. The Tanδ peak of the GO/PVDF composite films that was prepared by cosolvent method has higher intensity than the corresponding peak for the composite films prepared solely with DMF. This can be ascribed to the deionized water that makes GO better dispersed in the composite films, and the combination between GO and PVDF is reinforced, resulting in the increase of film's toughness.

SEM Analysis

To investigate the influence of GO on the microstructure of the composite films, SEM of GO/PVDF films cross-sections were obtained.

Figure 6(a) shows the microstructure of pure PVDF, where it can be seen that the morphology of pure PVDF layer is dense, smooth with no voids, but small fold lines appear on the surface. Compared with pure PVDF, the GO/PVDF composite films contain some granular aggregates and much grainy materials distributed in a gradient inhomogeneously dispersed, where the surface of the crystal is uneven. As seen from Figure 6(B1-B4), as the content of GO in the film increase from 0.04% to 0.1%, the grainy aggregates increase and its size also grows and more voids structures are observed. This phenomenon can be interpreted as follows: GO particles are dispersed inhomogeneously in the PVDF matrix and the microstructure of PVDF was destroyed as the increasing amount of GO resulted in the formation of large grainy aggregations.

Figure 6(c) shows the GO/PVDF composite films prepared using the cosolvent method, when compared with the Figure 6(B4), because the GO has a higher affinity for water than DMF, the cosolvent method helps to dispersed GO more evenly in PVDF matrix, which is attributed to the smoothness of fracture surface, the lower amount and smaller size of the grainy aggregations. The improved compatibility and interfacial activity between the GO and PVDF, dramatically improves the nanocomposites performance.

The result of Energy Dispersive Spectrometer (EDS) test is used to identify the elemental composition. Figure 7 shows the EDS of the grainy aggregates on the GO/PVDF composite films and the principal constituents of the composite and their percentages. The EDS results indicate that the composite films were composed of carbon, oxygen, and fluorine elements. The carbon elements and oxygen elements are attributable to the oxygen functional groups in GO, part of carbon elements from the PVDF, and fluorine elements is obviously from the C—F bonds of the PVDF.

Dielectric Properties Analysis

The dielectric properties of samples were measured in a frequency range between 10^{-2} and 10^{-7} Hz at a room temperature. Figures 8 and 9 shows the dielectric constant and dielectric loss of the pure PVDF and GO/PVDF nanocomposites.

As can be seen in Figure 8, the pure PVDF, exhibits a dielectric constant that is generally about 10 at a the frequency 10^{-2} Hz. With the increase in frequency, the dielectric constant of the material exhibits an obvious downward trend. In the frequency range between 10^{-1} Hz and 10^{5} Hz, the dielectric constant decreased slowly. When the frequency was increased to 10^{7} Hz, dielectric constant decreased to about 3.

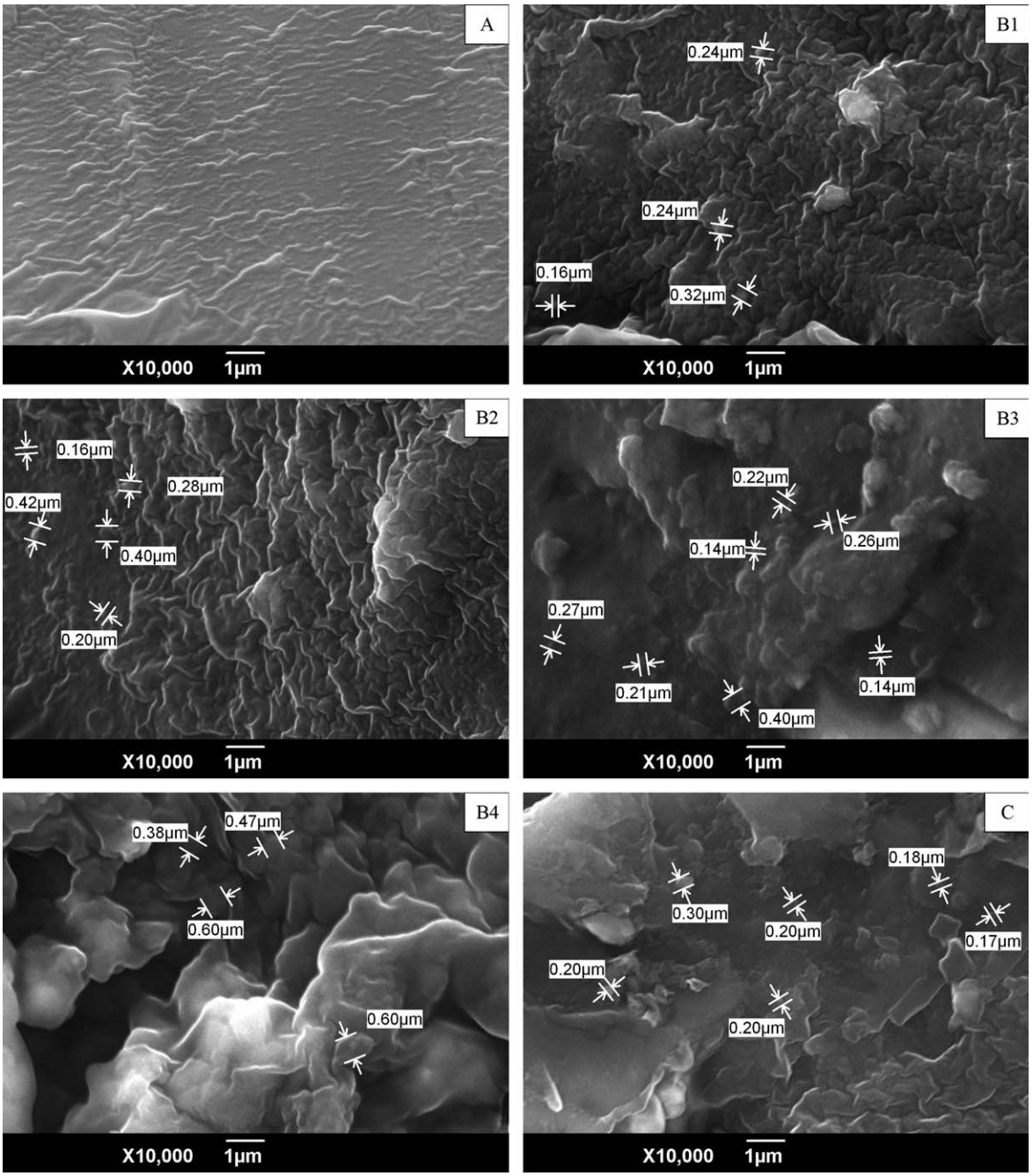

Figure 6. SEM of GO/PVDF composite films with (A) 0, (B1) 0.04, (B2) 0.06, (B3) 0.08, (B4) 0.10, and (C) 0.10 (cosolvent method DMF+ water) wt % GO.

By adding GO with a mass fraction of 0.04% and 0.06%, the dielectric constant of the composite changes only a little, reached about 11. When the content of GO is 0.08%, the dielectric constant of the composite is increased to 16 at the frequency of 10^{-2} Hz. When the GO content was 0.1%, the dielectric constant of the composite obvious improved, as showed in curve B4, which attained a reading of 23.

Under the same test conditions with the GO content of 0.1%, as shown in curve C, the composites prepared using the cosolvent method showed an improvement in dielectric constant above that of the composites prepared with DMF, almost reached 24.

There are two explanations for this phenomenon. First, compared with A, B1, B2, B3, B4, such improvement of dielectric constant may be correlated to the increasing GO content, the increased content of β-phase crystal enhanced the polarity, it may be the main reasons for the improving dielectric constant.

Compared with B4 and C, the main reasons for the improved dielectric constant may be the dispersion and networking of

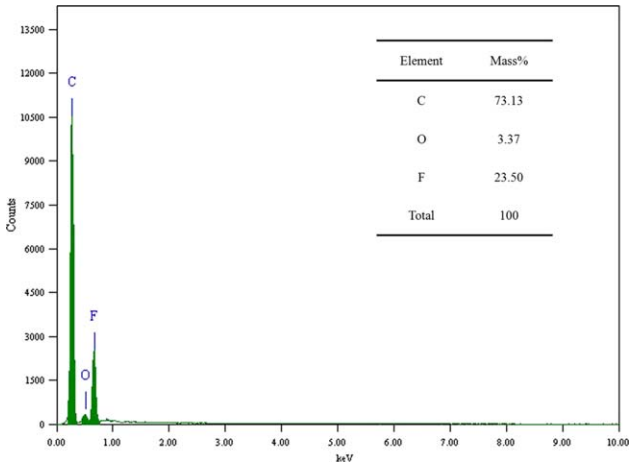

Figure 7. EDS of GO/PVDF composite films. [Color figure can be viewed in the online issue, which is available at wileyonlinelibrary.com.]

GO. The GO disperses much better in water whereas it forms less stable solutions in organic solvents such as DMF. Less sonication time is required to achieve good dispersion in water due to the hydrogen bonds that appeared to be more hydrophilic, which form between water and GO's functional groups.

GO is a material exhibits semiconducting properties, while GO dispersed in PVDF matrix, part of the GO structure may act as the role of tiny capacitors in the composite material, which leads to an increase in the dielectric constant of the composite.

The dielectric loss is a measurement of the energy dissipation from the movement or rotation of the molecules in the alternative electric field.[7] Figure 9 shows the changes of dielectric loss with frequency in a range between 10^{-2} and 10^{-7} Hz at room temperature. The dielectric loss of pure PVDF is 0.3 at the frequency of 10^{-2} Hz, but after addition of GO, the dielectric loss of composite material was increased. By adding different mass fractions of GO, the effect on the dielectric loss is basically the same, in between 4.5 and 5. By the graph, it is evident that the valley location of the dielectric loss curve does not substantially change with the different content of GO, which is due to this groups of samples that were prepared from the same substrate-PVDF matrix.

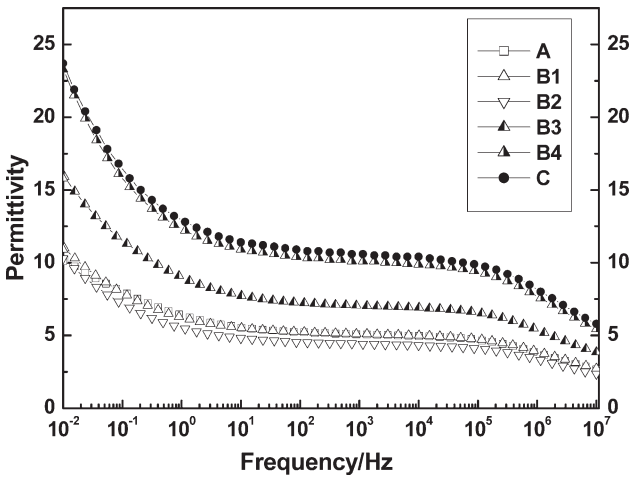

Figure 8. The dielectric constant under different frequency of GO/PVDF composite films with (A) 0, (B1) 0.04 (B2) 0.06, (B3) 0.08, (B4) 0.10, and (C) 0.10 (cosolvent method DMF+ water) wt % GO.

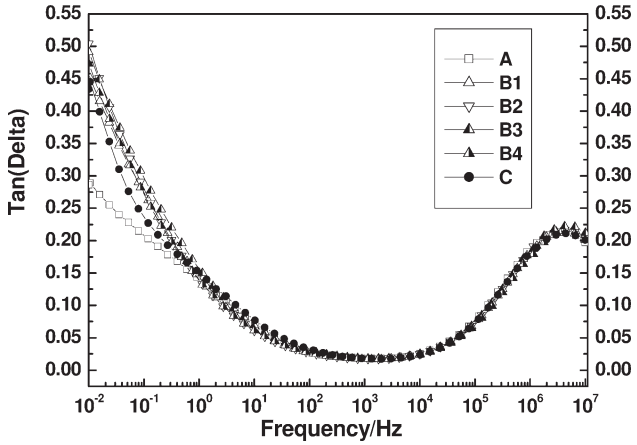

Figure 9. The dielectric loss under different frequency of GO/PVDF composite films with (A) 0, (B1) 0.04 (B2) 0.06, (B3) 0.08, (B4) 0.10, and (C) 0.10 (cosolvent method DMF+ water) wt % GO.

With the addition of GO, more interfacial area is created and the PVDF polymer chains are separated into smaller domains where more molecules or dipoles can rotate. Moreover, part of GO agglomerated in the PVDF matrix causing clustering of the free charge, which formed the electric conduction loss, which dissipated more energy.

As curve C shown, the dielectric loss of the GO/PVDF composite films prepared using the cosolvent method declined compared with curve B4, because the GO has a higher affinity for water than DMF, with the addition of deionized water, GO is well dispersed in the PVDF matrix, so the interface combination degree between PVDF and GO has improved, to a certain extent, the formation of aggregate is reduced, leading to the decrease of dielectric loss.

CONCLUSIONS

In summary, we have described the preparation of GO and GO/PVDF composite films. XRD and FTIR analysis showed that the crystal structure of the GO/PVDF composite films is the β-phase. Dielectric spectrum analysis revealed that the β-phase crystal structure could enhance the dielectric constant of the composite films. The dielectric constant and dielectric loss increased with the increasing GO loading throughout the whole frequency range, especially when the amount of GO was 0.1%, the dielectric constant of the composite film increased significantly that almost reached 24. Additionally, by observing the GO/PVDF composite films prepared using the cosolvent (deionized water/DMF) method, the β-phase in crystal appeared to increase and the dielectric constant improved significantly, with low dielectric loss. The SEM analysis of the microscopic surface of GO/PVDF composite films prepared by the cosolvent method showed a relatively smooth morphology, the amount and size of grainy aggregations in films were observed to be less. This result indicates the potential of using the cosolvent method for the synthesis of GO/PVDF nanocomposites involving deionized

water and DMF that yields well-dispersed GO in the PVDF matrix.

ACKNOWLEDGMENTS

The authors acknowledge the financial supports provided by the National Natural Science Foundation of China (Grant No. 51172180, 51305347 and 51372200), Program for New Century Excellent Talents in University of Ministry of Education of China (Grant No. NCET-12-1045), Local Service Program of Shaanxi Provincial Education Department (Grant No. 2013JC19), Specialized Research Fund for the Doctoral Program of Higher Education (Grant No. 20136118120003) and the Natural Science Foundation of Shaanxi Province (Grant No. 2014JQ7230).

REFERENCES

1. Kim, D. H.; Kim, B.; Kang, H. *Microsyst Technol.* **2004**, *10*, 275.
2. Indra-Devi, P.; Sivabharathy, M.; Ramachandran, K. *Optik* **2013**, *124*, 3872.
3. Ma, D. Z. The Polymer Structure and Performance; Science Press: Beijing, **1995**.
4. Hu, J.; Liu, B. L.; Wang, D. Q. *Polym. Bull.* **2003**, *27*, 63.
5. Tao, M. M.; Liu, F.; Ma, B. R.; Xue, L. X. *Desalination* **2013**, *316*, 137.
6. Ei-Achaby, M.; Arrakhiz, F. Z.; Vaudreuil, S.; Essassi, E. M.; Qaiss, A. *Appl. Surf. Sci.* **2012**, *258*, 7668.
7. Tang, C. W.; Li, B.; Sun, L. L.; Lively, B.; Zhong, W. H. *Eur. Polym. J.* **2012**, *48*, 1062.
8. Bormashenko, Y.; Pogreb, R.; Stanevsky, O.; Bormashenko, E. *Polym Test.* **2004**, *23*, 791.
9. Fukada, E.; Furukawa, T. *Ultrasonics* **1981**, *19*, 31.
10. Kim, N. K.; Lin, R. T.; Fakirov, S.; Aw, K.; Bhattacharyya, D. *Int. J. Polym. Mater Polym. Biomater.* **2014**, *63*, 23.
11. Zhu, G. D.; Zeng, Z. G.; Zhang, L.; Yan, X. J. *Comp. Mater. Sci.* **2008**, *44*, 224.
12. Liao, K. H.; Mittal, A.; Bose, S.; Leighton, C.; Andre-Mkhoyan, K.; Macosko, C. W. *ACS Nano* **2011**, *5*, 1253.
13. Mei, X. G.; Ouyang, J. Y. *Carbon* **2011**, *49*, 5389.
14. Sun, L.; Fugetsu, B. S. *Mater. Lett.* **2013**, *109*, 207.
15. Martins, P.; Caparros, C.; Goncalves, R.; Martins, P. M.; Benelmekki, M.; Botelho, G.; Lanceros-Mendez, S. *J. Phys. Chem. C* **2012**, *116*, 15790.
16. Layek, R. K.; Samanta, S.; Chatterjee, D. P.; Nandi, A. K. *Polymer* **2010**, *51*, 5846.
17. Song, H. S.; Liu, D. B. *Chem. Eng.* **2011**, *191*, 1.
18. Wang, Z. H.; Yu, H. R.; Xia, J. F.; Zhang, F. F.; Li, F.; Xia, Y. Z.; Li, Y. H. *Desalination* **2012**, *299*, 50.
19. Kuwahara, Y.; Ueyama, M.; Yagi, R.; Koinuma, M.; Ogata, T.; Kim, S.; Matsumoto, Y.; Kurihara, S. *Mater. Lett.* **2013**, *108*, 308.
20. Nirmal, S.; Zoubeida, O.; Greg, E.; Henry, S. In: Proceedings of Society of Photo-Optical Instrumentation Engineers, Preparation of reduced Graphene/PVDF nanocomposites using co-solvent approach, California, **2012**, p 1.
21. Chae, H. K.; Siberio-Perez, D. Y.; Kim, J.; Yongbok, G.; Eddaoudi, M.; Matzger, A. J.; Michael, O.; Yaghi, O. M. *Nature* **2004**, *427*, 523.
22. Salimi, A.; Yousefi, A. A. *Polym. Test.* **2003**, *22*, 699.
23. Bachmann, M. A.; Gordon, W. L.; Koenig, J. L.; Lando, J. B. *J. Appl. Phys.* **1979**, *50*, 6106.
24. Shah, D.; Maiti, P.; Gunn, E.; Schmidt, D. F.; Jiang, D. D.; Batt, C. A.; Giannelis, E. P. *Adv. Mater.* **2004**, *16*, 1173.
25. Arrouvel, C.; Digne, M.; Breysse, M.; Toulhoat, H.; Raybaud, P.; Catal, J. **2004**, *222*, 152.
26. Becker, T. M.; Bauer, J. A. K.; Bene, J. E. D.; Orchin, M.; Organomet, J. *Chemistry* **2001**, *629*, 165.